


[Title]

Serial profiling of circulating tumor DNA for optimization of anti-VEGF chemotherapy in metastatic colorectal cancer patients

[Short title]

Serial profiling of ctDNA during anti-VEGF therapy

[Authors]

Masami Yamauchi^{1,2} , Yuji Urabe^{2,3}, Atsushi Ono^{2,5}, Daiki Miki^{4,5}, Hidenori Ochi^{2,4,5}, Kazuaki Chayama^{2,4,5}

¹ **Division of Clinical Oncology, Hiroshima Prefectural Hospital, Hiroshima, Japan.**

² **Department of Gastroenterology and Metabolism, Institute of Biomedical and Health Sciences, Graduate School of Biomedical and Health Sciences, Hiroshima University, Hiroshima, Japan.**

³ **Department of Regeneration and Medicine Medical Center for Translation and Clinical Research, Hiroshima University Hospital, Hiroshima, Japan.**

⁴ **Laboratory for Liver Diseases, SNP Research Center, Institute of Physical and Chemical Research (RIKEN), Hiroshima, Japan.**

⁵ **Liver Research Project Center, Hiroshima University, Hiroshima, Japan.**

[Corresponding author]

Kazuaki Chayama, Department of Gastroenterology and Metabolism, Applied Life Sciences, Institute of Biomedical and Health Sciences, Hiroshima University

This article has been accepted for publication and undergone full peer review but has not been through the copyediting, typesetting, pagination and proofreading process which may lead to differences between this version and the Version of Record. Please cite this article as an 'Accepted Article', doi: 10.1002/ijc.31154

1-2-3 Kasumi, Minami-ku, Hiroshima 734-8551, Japan

E-mail: chayama@hiroshima-u.ac.jp; Fax: +81 82 255 6220

[Keywords]

circulating tumor DNA; colorectal cancer; chemotherapy; VEGF

[Abbreviations]

ctDNA, circulating tumor DNA; MAF, mutant allele frequency; mFOLFOX6, folinic acid, 5-fluorouracil, and oxaliplatin; CapeOX, capecitabine, oxaliplatin.

[Appropriate article category]

Tumor Markers and Signatures

[Brief description]

Tracking tumor genotype during anti-VEGF chemotherapy for treatment optimization in metastatic colorectal cancer has been a major challenge. We investigated changes in the amount and constitution of circulating tumor DNA (ctDNA) in serial peripheral blood samples during chemotherapy. It may provide information about disease control and survival prediction. ctDNA that is newly detected after therapy could provide clues to uncovering the mechanism of resistance to angiogenesis inhibitors.

Abstract

Understanding the molecular changes in tumors in response to anti-VEGF chemotherapy is crucial for optimization of the treatment strategy for metastatic colorectal cancer. We prospectively investigated changes in the amount and constitution of circulating tumor DNA (ctDNA) in serial peripheral blood samples during chemotherapy. Sixty-one plasma samples taken at different time points (baseline, remission, and post-progression) and pre-treatment tumor samples were collected from 21 patients who received bevacizumab-containing first-line chemotherapy. Extracted DNA was sequenced by next-generation sequencing using a panel of 90 oncogenes. Candidate ctDNAs in plasma were validated using mutational data from matching tumors. ctDNAs encoding one to six trunk mutations were found in all 21 cases, and the mutant allele frequency (MAF) was distributed over a wide range (1-89%). Significant decreases in the MAF at remission and increases in the MAF after progression were observed ($p < 0.001$). Reduction in the MAF to below 2% in the remission period was strongly associated with better survival (16.6 vs. 32.5 months, $P < 0.001$). In two cases, mutations (in *CREBBP* and *FBXW7* genes) were newly detected in ctDNA at a low frequency of around 1% in the post-progression period. The use of ctDNA allows elucidation of the tumor clonal repertoire and tumor evolution during anti-VEGF chemotherapy. Changes in ctDNA levels could be useful as predictive biomarkers for survival. Mutations newly detected in ctDNA in the late treatment period might reveal the rise of a minor tumor clone that may show resistance to anti-VEGF therapy.

Introduction

The combination of cytotoxic chemotherapeutics and targeted drugs has been regarded as the standard treatment for patients with metastatic colorectal cancer (mCRC).¹ Either addition of anti-epidermal growth factor receptor (EGFR) antibody or anti-vascular endothelial growth factor-A (VEGF-A) antibody to cytotoxic regimens has been demonstrated to improve survival.^{2,3} Despite remarkable advances in the development of therapies, the emergence of resistance eventually limits their effectiveness. For optimization of treatment strategies, further understanding of genetic events in patients during chemotherapy and the establishment of useful genomic biomarkers to guide the management of treatment are crucial.

Plasma circulating tumor DNA (ctDNA) has been increasingly investigated as a promising application for genomic profiling of tumors. Unlike repeated tumor biopsy, which is not feasible in clinical practice, analysis of ctDNA obtained from peripheral blood could be used to less-invasively track changes in the genetic composition of molecularly and cellularly heterogeneous tumors.^{4,5} Furthermore, it was demonstrated that longitudinal monitoring of ctDNA effectively detects the emergence of *RAS* gene mutations induced by anti-EGFR therapy in an initially *RAS*-wild population.^{6,7} These additional genomic aberrations might be associated with tumor clonal evolution and selection that may occur at distinct metastatic sites as a response to treatment pressure.^{8,}

In contrast, little is known about ctDNA kinetics or alterations in its makeup during anti-VEGF chemotherapy, which has been broadly adopted as one of the common first-line chemotherapies for mCRC. The lack of knowledge regarding novel tumor genetic events during chemotherapy has long restricted optimal patient selection for

anti-VEGF therapy.¹⁰ Angiogenesis inhibitors, such as bevacizumab, cause substantial therapeutic stress to tumor cells, primarily inducing hypoxic stress.¹¹ Long-term exposure to anti-angiogenic agents may affect tumor genomic composition or trigger selection of a hypoxia-tolerant minor subpopulation of tumor cells. Several studies have reported increased tumor invasiveness in response to anti-angiogenic therapies in animal models.^{12, 13} However, tracing tumor gene status during anti-VEGF chemotherapy in the clinical setting has been a major challenge.

The aim of this study was to explore molecular events that may be associated with treatment outcome or development of resistance during anti-VEGF chemotherapy. We investigated dynamic changes in the amount and constitution of ctDNA in serial plasma samples of patients who received standard anti-angiogenic chemotherapy.

Materials and Methods

Patients

Patients were recruited prospectively for this study from January 2014 to January 2016 at Hiroshima Prefectural Hospital in Hiroshima, Japan. The study population consisted of 61 serial peripheral blood samples, matched tumor samples, and peripheral blood leukocytes from 21 patients with mCRC. All patients were treated with bevacizumab-containing cytotoxic chemotherapy as the first-line treatment for at least six months. Clinicopathological features of the patients in this study are shown in **Supplementary Table 1**. Targeted next-generation sequencing (NGS) of DNA extracted from plasma samples, tumor tissues, and control lymphocytes identified somatic rearrangements. The Human Ethics Review Committees of Hiroshima University and Hiroshima Prefectural Hospital approved the study. All patients provided written informed consent.

Determination of time points for analysis

We set the following three time points for analysis of the samples: baseline (before the initiation of chemotherapy), remission, and post-progression. The timing of remission was determined by computed tomography (CT) findings with the most favorable response assessed using the Response Evaluation Criteria in Solid Tumors (RECIST) version 1.1 criteria. In patients COL-001 and COL-021, two different plasma specimens were analyzed at the time of remission. The timing of progression was determined by discontinuation of cytotoxic chemotherapy plus bevacizumab (the end of the first-line oxaliplatin-based therapy in COL-001, 026, 030, 034, 044, 046-060, or the end of the second-line irinotecan-based therapy in the other patients).

Baseline mutations within the archival tumor tissue

DNA of the primary tumor was extracted from five 10- μ m-thick slides that were made from the formalin-fixed paraffin embedded (FFPE) samples acquired at the time of initial diagnosis using the GeneRead DNA FFPE Kit (Qiagen, Germany). The quantity and quality of the FFPE-derived DNA samples were checked by calculation of the normalized DNA integrity score ($\Delta\Delta Cq$) that was assessed with qPCR using the Agilent NGS FFPE QC Kit (Agilent, United States).

Control lymphocytes

Seven milliliters of peripheral venous blood were collected prior to the initiation of chemotherapy. The genomic DNA of lymphocytes was extracted and used as germline controls.

Cell-free DNA

Ten milliliters of peripheral venous blood were collected using EDTA as an anticoagulant at baseline, remission, and post-progression. The drawn blood was immediately processed to isolate plasma by a two-step centrifugation process: 3500 rpm, for 10 minutes followed by 12000 rpm for 10 minutes at 4 °C. Separated plasma was stored at -80 °C prior to DNA extraction. Cell-free DNA was purified from 3 ml of plasma aliquots using QIAGEN Plasmid Plus Kits (Qiagen) according to the manufacturer's protocols. Cell-free DNA was eluted into 100 μ l of buffer, quantified using Qubit HS (Thermo Fisher Scientific, US), and stored at 4 °C.

Target enrichment and next-generation sequencing

Cell-free DNA and DNA extracted from primary tumors and normal lymphocytes was fragmented and used for library construction according to the manufacturer's instructions. In all cases, 40 ng of cell-free DNA was prepared for sequencing. The exons of 90 oncogenes and the associated introns of 35 fusion oncogenes were enriched

using the KAPA Hyperprep kit and the NCC oncopanel (Agilent, **Supplementary Table 2**). The resulting pooled libraries were quality control checked using the High Sensitivity D1000 ScreenTape System with the 2200 TapeStation Instrument (Agilent). Sequencing was performed with paired-end reads on the HiSeq 2500 platform (Illumina, US).

Variant Detection

Sequencing reads were aligned to the hg19/GRCh37 reference sequence and analyzed using the CLC Genomics Workbench (CLC bio, Denmark). PCR duplicates were removed and local realignment was performed using CLC to improve mapping quality prior to variant calling. To identify variants in plasma and primary tumor samples, the low frequency variant detection software in CLC was used. Called variants were considered germline mutations if they were called in the control lymphocytes or were found in the dbSNP 137 database, the HapMap database, or the 1000 Genomes Project.

The remaining mutations in plasma samples were considered ctDNA candidates. To reduce the false positive rate, we set the cutoff values for ctDNA in plasma as follows: read depth > 200; number of mutant reads > 18; allele frequency of mutant reads > 0.5%; average quality > 20; and the ratio of forward reads to reverse reads > 10%.

Identified ctDNAs were validated by detection of mutations in the sequence of matching primary tumor samples.

Disease burden and tumor markers

CT was performed at least bimonthly and disease response was evaluated by RECIST version 1.1. Tumor burden was calculated from a CT image using the sum of the diameters (longest for non-nodal lesions, short axis for nodal lesions) of one or two of the largest lesions in each metastatic site. The levels of serum carcinoembryonic antigen

(CEA) and serum carbohydrate antigen 19-9 (CA19-9) were measured monthly. The maximum intervals between sampling of ctDNA and CT assessment or measurement of tumor markers were four weeks or two weeks, respectively.

Statistical analysis

The differences in mutant allele frequency at baseline and remission, or at remission and post-progression, were assessed using the Wilcoxon signed-rank test. Correlations between the variables were assessed using Spearman's rank correlation. Overall survival was estimated using Kaplan-Meier methods and differences between subgroups were evaluated using the log-rank test. Univariate and multivariate Cox regression analyses were performed for background clinicopathological parameters (age, sex, location of the primary tumor, number of metastatic organs, CEA, CA19-9, *RAS* status, and tumor burden) and mutant allele frequency. Comparisons were considered significant if the *P*-value was less than 0.05. All statistical analyses were performed using R version 3.3.1.

Results

Constitution and dynamics of the ctDNA

In all 21 cases, ctDNA containing one to six somatic mutations per patient was identified in plasma samples at baseline (**Figure 1**). In the sequencing analysis, the coverage depth in targeted regions after the removal of PCR duplicates ranged from 888 to 5449. Out of 52 ctDNAs identified at baseline, 30 (58%) were single nucleotide variants and 22 (42%) were nucleotide insertions or deletions (**Table 1**). No actionable gene fusions were detected. There was some diversity in the ctDNAs in terms of the cellular processes/signaling pathways with which the corresponding genes are known to be involved, and this diversity may underlie in part the molecular characterization of each tumor.

The concentration of ctDNA, which was determined based on assessment of the mutant allele frequency (MAF), fluctuated dynamically throughout the treatment period.

Significant decreases in the MAF at remission by chemotherapy and increases in the MAF after disease progression that were accompanied by the appearance of resistance to chemotherapy were observed (**Figure 2**). Of the 52 ctDNAs identified at baseline, 48 ctDNAs were detectable post-progression; the four mutations that were not detected post-progression were *APC* in patient COL-023, *SETD2* and *ARID1A* in patient COL-025, and *APC* in patient COL-058.

ctDNA, tumor burden, and tumor markers

There was a positive correlation between the MAF and tumor load; however, this correlation was diminished when the MAF and tumor burden data were limited to the time of remission (**Figure 3A**). On the other hand, there were no correlations between the MAF and tumor markers at any time points (**Figure 3B, Figure 3C**). In addition, the

levels of CEA and CA19-9 were not elevated at any time point in three patients (COL-023, COL-025, COL-030).

ctDNA as a predictive biomarker for survival

Reduction in the MAF to below the median value in the remission period was strongly associated with better survival (16.6 vs. 32.5 months, $p < 0.001$, **Figure 4**). Even in the cases in which the patient had multiple ctDNAs, the MAF had decreased to less than 2% in the long-term survivors. The MAF at remission was an independent predictor for survival following multivariate Cox regression analysis adjusted by clinicopathological parameters (**Supplementary Table 3**). Although higher MAF at baseline seemed to be associated with worse survival, an appropriate MAF threshold was not found because of the wide distribution and variability of MAFs among the cases. The median duration between treatment initiation and plasma sampling at remission was 4.5 months in the MAF $< 2\%$ group and 4 months in the MAF $\geq 2\%$ group.

Of note, despite the relatively high MAFs at baseline in patient COL-001 (**Figure 5**), ctDNA had become undetectable in response to bevacizumab-containing chemotherapy, whereas only a moderate decline in tumor markers was observed. The MAFs had rebounded to a high level at the post-progression time point; however, the subsequent EGFR-blockade chemotherapy and successful resection of liver metastases indeed prolonged the patient's survival for up to 32.5 months.

Mutations newly detected at post-progression

In two patients, we detected a mutation at a low frequency of around 1% in the post-progression period (**Figure 6**). In one patient, a mutation in the cAMP-response element-binding protein-binding protein gene (*CREBBP*) emerged after concentrated exposure to bevacizumab-containing chemotherapy. This patient already showed a

truncal mutation in *MET* from baseline, for which the level mirrored the disease control.

In the other patient, COL-034, mutation of the F-box and WD repeat domain-containing gene (*FBXW7*) was detected for the first time in the late treatment period. This patient already showed mutations in four other genes with respect to baseline.

Accepted Article

Discussion

The present study demonstrated in several ways the utility of serial sampling of ctDNA over a long clinical course in terms of guiding anti-VEGF therapy for mCRC. Targeted NGS of plasma DNA may be sufficient to provide information about tumor genotype, to monitor disease control, and to predict survival. ctDNA that is newly detected after therapy could provide clues to uncovering the mechanism of resistance to angiogenesis inhibitors.

We first showed the simple dynamics of ctDNA over the long-term clinical course, in which the level of ctDNA declined in response to chemotherapy and thereafter increased again, suggesting the acquisition of resistance. The most recent ctDNA study,¹⁴ which employed a multiregional approach and a large cancer panel, indicated that ctDNA detection displayed high sensitivity and accuracy for the molecular assessment of pancreatic cancer, confirming that ctDNA analysis is a feasible method for tumor analysis. High levels of truncal ctDNAs that represent the DNA mutations in the majority of tumor cells¹⁵ are suitable for monitoring tumors during follow-up without drop out. In most of the previous landmark reports, the genes that were screened were limited to the area of interest and were associated with the *RAS-RAF-MAPK* signaling pathway.^{16, 17} Furthermore, reported ctDNA data represented only a cross-section of ctDNAs present at the initial diagnosis¹⁸ or at post-treatment.¹⁶ Our less-biased NGS approach to identification of ctDNAs indicates that wide-spectrum, longitudinal ctDNA analysis may be a promising quantitative measurement method for monitoring disease. It is also expected that this approach may provide an alternative to the measurement of tumor markers, which often do not accurately reflect disease status due to lack of sensitivity and specificity.¹⁹

Next, we focused on determination of whether the level of ctDNA at remission could be a biomarker for patient survival. A recent study showed a trend for longer progression-free survival in patients with mCRC who experienced a 10-fold or greater decrease in ctDNA at the end of the first cycle of chemotherapy compared to baseline.¹⁸

This early indicator of survival should certainly be regarded as a valuable survival indicator. However, chemotherapy for mCRC is so effective in the first-line setting that it generally continues for over half a year and sometimes it is integrated with other procedures including surgery. We therefore considered that analysis of the ctDNA level at a later phase accompanied by the most favorable therapeutic response would be a more practical and reasonable indicator for optimization of treatment. Although the mechanism of ctDNA release from a tumor is not fully understood, it has been strongly suggested that it is related to tumor cell apoptosis.²⁰ We consider that a decreased level of ctDNA may be linked to a “silent” status of the tumor that reflects not only suppression of cancer cell growth but also suppression of apoptosis. It is likely that the degree of the decrease in ctDNA might be a surrogate for the depth of the tumor response to therapy.²¹

Finally, we proposed a model in which newly detected mutations at the “post-progression” time point might explain acquired resistance to hypoxic conditions under anti-VEGF therapy. One of these newly detected mutations, p.R1347W, is located in the coding exon 31 of *CREBBP*, which is part of the histone acetyltransferase (HAT) domain that plays a pivotal role in the maintenance of cellular epigenetic equilibrium.²² HAT missense mutations can lead to a histone deacetylase dominant condition, gene silencing, and consequent tumorigenesis.^{23, 24} The second newly identified mutation, p.H455Q, occurs inside a WD-40 domain. Mutations in WD-40 domains are thought to

interfere with the function of the tumor suppressor FBXW7 protein, which functions as a component of ubiquitin ligase.²⁵ Loss of FBXW7 function reduces turnover of oncogenic substrates such as MYC, Notch,²⁶ and ENO1,²⁷ which confers metabolic advantages to tumor cells under hypoxic conditions. A previous study reported that mutant *RAS* alleles that were newly detected after disease progression in mCRC that became refractory to anti-EGFR antibody were distributed at a very low concentration (0.02-10%).¹⁷ It was possible to detect most of these mutations by using supersensitive assays such as BEAMing¹⁷ or digital PCR.²⁸ It is unclear why the levels of ctDNA derived from actively resistant lesions are present at such a low concentration. However, the observed frequency of private mutations of around 1% in our study could be evidence of clonal selection under treatment pressure. Compared to a previous report in which the sensitivity of ctDNA detection was unsatisfactory,²⁹ our careful patient selection, prompt plasma isolation (< 30 minutes), and strict algorithm to exclude sequencing errors should ensure the detection of low frequency ctDNAs.

Although we have not carried out functional validation of the late-emerging ctDNA mutations found in our study, there have been a number of reports that showed the importance of both *CREBBP*^{30, 31} and *FBXW7*^{32, 33} as tumor suppressor genes by using knockdown experiments in various cancer cell lines or animal-cancer models. Our hypothesis regarding the association of *CREBBP* or *FBXW7* mutation with tolerance to hypoxia is consistent with the cancer biology demonstrated in those studies. Since resistance mechanisms are thought to be specific to individual patients, we think that further accumulation of newly detected mutations in a larger cohort is important.

Our pilot study has several limitations. Although sample collection was performed prospectively and the collected blood volume of 10 ml was sufficient for analysis, the

sample size was small. To clarify the correlation of ctDNA and treatment effect, patients without beneficial response to anti-VEGF therapy were excluded. Therefore, it is unclear whether a similar comprehensive approach might be feasible for patients with oligometastatic lesions or patients with intrinsic resistance. The second limitation is the absence of a control arm. The exposure to chemotherapy without targeted drugs may in fact alter the mutational status of the tumor.³⁴ Since bevacizumab is always used in combination with chemotherapeutics, inspection of gene alteration limited to the effect of bevacizumab administration alone is not possible and would be meaningless in the clinical setting. In the near future, technological advances will allow frequent ctDNA analyses during therapy with reasonable costs. Prospective trials with proper treatment stratification and with adequate power for statistical analysis are warranted to overcome these limitations.³⁵

In conclusion, we proposed the use of ctDNA as a biomarker for a patient population that has not been tested in previous studies. We believe that accumulation of genetic information obtained by serial ctDNA profiling could contribute to the construction of precision medicine for patients with mCRC.

Acknowledgments

This work was supported by the Program of the network-type Joint Usage/Research Center for Radiation Disaster Medical Science of Hiroshima University, Nagasaki University, and Fukushima Medical University.

References

1. Fakih MG. Metastatic colorectal cancer: current state and future directions. *J Clin Oncol* 2015; 33: 1809-24.
2. Van Cutsem E, Köhne CH, Láng I, Folprecht G, Nowacki MP, Cascinu S, Shchepotin I, Maurel J, Cunningham D, Tejpar S, Schlichting M, Zobel A, Celik I, Rougier P, Ciardiello F. Cetuximab plus irinotecan, fluorouracil, and leucovorin as first-line treatment for metastatic colorectal cancer: updated analysis of overall survival according to tumor KRAS and BRAF mutation status. *J Clin Oncol* 2011; 29: 2011-9.
3. Hurwitz H, Fehrenbacher L, Novotny W, Cartwright T, Hainsworth J, Heim W, Berlin J, Baron A, Griffing S, Holmgren E, Ferrara N, Fyfe G, Rogers B, Ross R, Kabbinavar F. Bevacizumab plus irinotecan, fluorouracil, and leucovorin for metastatic colorectal cancer. *N Engl J Med* 2004; 350: 2335-42.
4. Diaz LA Jr, Bardelli A. Liquid biopsies: genotyping circulating tumor DNA. *J Clin Oncol* 2014; 32: 579-86.
5. Russo M, Siravegna G, Blazkowsky LS, Corti G, Crisafulli G, Ahronian LG, Mussolin B, Kwak EL, Buscarino M, Lazzari L, Valtorta E, Truini M, Jessop NA, Robinson HE, Hong TS, Mino-Kenudson M, Di Nicolantonio F, Thabet A, Sartore-Bianchi A, Siena S, Iafrate AJ, Bardelli A, Corcoran RB. Tumor Heterogeneity and Lesion-Specific Response to Targeted Therapy in Colorectal Cancer. *Cancer Discov* 2016; 6: 147-53.
6. Diaz LA Jr, Williams RT, Wu J, Kinde I, Hecht JR, Berlin J, Allen B, Bozic I, Reiter JG, Nowak MA, Kinzler KW, Oliner KS, Vogelstein B. The molecular evolution of acquired resistance to targeted EGFR blockade in colorectal cancers.

- Nature 2012; 486: 537-40.
7. Misale S, Yaeger R, Hobor S, Scala E, Janakiraman M, Liska D, Valtorta E, Schiavo R, Buscarino M, Siravegna G, Bencardino K, Cercek A, Chen CT, Veronese S, Zanon C, Sartore-Bianchi A, Gambacorta M, Gallicchio M, Vakiani E, Boscaro V, Medico E, Weiser M, Siena S, Di Nicolantonio F, Solit D, Bardelli A. Emergence of KRAS mutations and acquired resistance to anti-EGFR therapy in colorectal cancer. *Nature* 2012; 486: 532-6.
 8. Murtaza M, Dawson SJ, Tsui DW, Gale D, Forshew T, Piskorz AM, Parkinson C, Chin SF, Kingsbury Z, Wong AS, Marass F, Humphray S, Hadfield J, Bentley D, Chin TM, Brenton JD, Caldas C, Rosenfeld N. Non-invasive analysis of acquired resistance to cancer therapy by sequencing of plasma DNA. *Nature* 2013; 497: 108-12.
 9. Bettegowda C, Sausen M, Leary RJ, Kinde I, Wang Y, Agrawal N, Bartlett BR, Wang H, Luber B, Alani RM, Antonarakis ES, Azad NS, Bardelli A, Brem H, Cameron JL, Lee CC, Fecher LA, Gallia GL, Gibbs P, Le D, Giuntoli RL, Goggins M, Hogarty MD, Holdhoff M, Hong SM, Jiao Y, Juhl HH, Kim JJ, Siravegna G, Laheru DA, Lauricella C, Lim M, Lipson EJ, Marie SK, Netto GJ, Oliner KS, Olivi A, Olsson L, Riggins GJ, Sartore-Bianchi A, Schmidt K, Shih IM, Oba-Shinjo SM, Siena S, Theodorescu D, Tie J, Harkins TT, Veronese S, Wang TL, Weingart JD, Wolfgang CL, Wood LD, Xing D, Hruban RH, Wu J, Allen PJ, Schmidt CM, Choti MA, Velculescu VE, Kinzler KW, Vogelstein B, Papadopoulos N, Diaz LA Jr. Detection of circulating tumor DNA in early- and late-stage human malignancies. *Sci Transl Med* 2014; 6: 224ra24.
 10. Moserle L, Jiménez-Valerio G, Casanovas O. Antiangiogenic therapies: going

- beyond their limits. *Cancer Discov* 2014; 4: 31-41.
11. Goel HL, Mercurio AM. VEGF targets the tumour cell. *Nat Rev Cancer* 2013; 13: 871-82.
 12. Pàez-Ribes M, Allen E, Hudock J, Takeda T, Okuyama H, Viñals F, Inoue M, Bergers G, Hanahan D, Casanovas O. Antiangiogenic therapy elicits malignant progression of tumors to increased local invasion and distant metastasis. *Cancer Cell* 2009; 15: 220-31.
 13. Ebos JM, Lee CR, Cruz-Munoz W, Bjarnason GA, Christensen JG, Kerbel RS. Accelerated metastasis after short-term treatment with a potent inhibitor of tumor angiogenesis. *Cancer Cell* 2009; 15: 232-9.
 14. Takai E, Totoki Y, Nakamura H, Morizane C, Nara S, Hama N, Suzuki M, Furukawa E, Kato M, Hayashi H, Kohno T, Ueno H, Shimada K, Okusaka T, Nakagama H, Shibata T, Yachida S. Clinical utility of circulating tumor DNA for molecular assessment in pancreatic cancer. *Sci Rep* 2015; 5: 18425.
 15. Murtaza M, Dawson SJ, Pogrebniak K, Rueda OM, Provenzano E, Grant J, Chin SF, Tsui DW, Marass F, Gale D, Ali HR, Shah P, Contente-Cuomo T, Farahani H, Shumansky K, Kingsbury Z, Humphray S, Bentley D, Shah SP, Wallis M, Rosenfeld N, Caldas C. Multifocal clonal evolution characterized using circulating tumour DNA in a case of metastatic breast cancer. *Nat Commun* 2015; 6: 8760.
 16. Siravegna G, Mussolin B, Buscarino M, Corti G, Cassingena A, Crisafulli G, Ponzetti A, Cremolini C, Amatu A, Lauricella C, Lamba S, Hobor S, Avallone A, Valtorta E, Rospo G, Medico E, Motta V, Antoniotti C, Tatangelo F, Bellosillo B, Veronese S, Budillon A, Montagut C, Racca P, Marsoni S, Falcone A, Corcoran RB, Di Nicolantonio F, Loupakis F, Siena S, Sartore-Bianchi A, Bardelli A. Clonal

- evolution and resistance to EGFR blockade in the blood of colorectal cancer patients. *Nat Med* 2015; 21: 795-801.
17. Morelli MP, Overman MJ, Dasari A, Kazmi SM, Mazard T, Vilar E, Morris VK, Lee MS, Herron D, Eng C, Morris J, Kee BK, Janku F, Deaton FL, Garrett C, Maru D, Diehl F, Angenendt P, Kopetz S. Characterizing the patterns of clonal selection in circulating tumor DNA from patients with colorectal cancer refractory to anti-EGFR treatment. *Ann Oncol* 2015; 26: 731-6.
18. Tie J, Kinde I, Wang Y, Wong HL, Roebert J, Christie M, Tacey M, Wong R, Singh M, Karapetis CS, Desai J, Tran B, Strausberg RL, Diaz LA Jr, Papadopoulos N, Kinzler KW, Vogelstein B, Gibbs P. Circulating tumor DNA as an early marker of therapeutic response in patients with metastatic colorectal cancer. *Ann Oncol* 2015; 26: 1715-22.
19. Nicholson BD, Shinkins B, Pathiraja I, Roberts NW, James TJ, Mallett S, Perera R, Primrose JN, Mant D. Blood CEA levels for detecting recurrent colorectal cancer. *Cochrane Database Syst Rev* 2015; 12: CD011134.
20. Thierry AR, Mouliere F, Gongora C, Ollier J, Robert B, Ychou M, Del Rio M, Molina F. Origin and quantification of circulating DNA in mice with human colorectal cancer xenografts. *Nucleic Acids Res* 2010; 38: 6159-75.
21. Heinemann V, Stintzing S, Modest DP, Giessen-Jung C, Michl M, Mansmann UR. Early tumour shrinkage (ETS) and depth of response (DpR) in the treatment of patients with metastatic colorectal cancer (mCRC). *Eur J Cancer* 2015; 51: 1927-36.
22. Glazak MA, Seto E. Histone deacetylases and cancer. *Oncogene* 2007; 26: 5420-32.

23. Pasqualucci L, Dominguez-Sola D, Chiarenza A, Fabbri G, Grunn A, Trifonov V, Kasper LH, Lerach S, Tang H, Ma J, Rossi D, Chadburn A, Murty VV, Mullighan CG, Gaidano G, Rabadan R, Brindle PK, Dalla-Favera R. Inactivating mutations of acetyltransferase genes in B-cell lymphoma. *Nature* 2011; 471: 189-95.
24. Zhang J, Vlasevska S, Wells VA, Nataraj S, Holmes AB, Duval R, Meyer SN, Mo T, Basso K, Brindle PK, Hussein S, Dalla-Favera R, Pasqualucci L. The CREBBP Acetyltransferase Is a Haploinsufficient Tumor Suppressor in B-cell Lymphoma. *Cancer Discov* 2017; 7: 322-337.
25. Lupini L, Bassi C, Mlcochova J, Musa G, Russo M, Vychytilova-Faltejskova P, Svoboda M, Sabbioni S, Nemecek R, Slaby O, Negrini M. Prediction of response to anti-EGFR antibody-based therapies by multigene sequencing in colorectal cancer patients. *BMC Cancer* 2015; 15: 808.
26. Welcker M, Clurman BE. FBW7 ubiquitin ligase: a tumour suppressor at the crossroads of cell division, growth and differentiation. *Nat Rev Cancer* 2008; 8: 83-93.
27. Zhan P, Wang Y, Zhao S, Liu C, Wang Y, Wen M, Mao JH, Wei G, Zhang P. FBXW7 negatively regulates ENO1 expression and function in colorectal cancer. *Lab Invest* 2015; 95: 995-1004.
28. Dawson SJ, Tsui DW, Murtaza M, Biggs H, Rueda OM, Chin SF, Dunning MJ, Gale D, Forshew T, Mahler-Araujo B, Rajan S, Humphray S, Becq J, Halsall D, Wallis M, Bentley D, Caldas C, Rosenfeld N. Analysis of circulating tumor DNA to monitor metastatic breast cancer. *N Engl J Med* 2013; 368: 1199-209.
29. Beije N, Helmijr JC, Weerts MJ, Beaufort CM, Wiggin M, Marziali A, Verhoef C, Sleijfer S, Jansen MP, Martens JW. Somatic mutation detection using various

Accepted Article

targeted detection assays in paired samples of circulating tumor DNA, primary tumor and metastases from patients undergoing resection of colorectal liver metastases. *Mol Oncol* 2016. pii: S1574-7891(16)30110-7.

30. Jiang Y, Ortega-Molina A, Geng H, Ying HY, Hatzi K, Parsa S, McNally D, Wang L, Doane AS, Agirre X, Teater M, Meydan C, Li Z, Poloway D, Wang S, Ennishi D, Scott DW, Stengel KR, Kranz JE, Holson E, Sharma S, Young JW, Chu CS, Roeder RG, Shaknovich R, Hiebert SW, Gascoyne RD, Tam W, Elemento O, Wendel HG, Melnick AM. CREBBP Inactivation Promotes the Development of HDAC3-Dependent Lymphomas. *Cancer Discov* 2017; 7: 38-53.
31. Dixon ZA, Nicholson L, Zeppetbauer M, Matheson E, Sinclair P, Harrison CJ, Irving JA. CREBBP knockdown enhances RAS/RAF/MEK/ERK signalling in Ras pathway mutated acute lymphoblastic leukaemia but does not modulate chemotherapeutic response. *Haematologica* 2016. pii: haematol.2016.145177.
32. Ibusuki M, Yamamoto Y, Shinriki S, Ando Y, Iwase H. Reduced expression of ubiquitin ligase FBXW7 mRNA is associated with poor prognosis in breast cancer patients. *Cancer Sci* 2011; 102: 439-45.
33. Wang Z, Inuzuka H, Zhong J, Wan L, Fukushima H, Sarkar FH, Wei W. Tumor suppressor functions of FBW7 in cancer development and progression. *FEBS Lett* 2012; 586: 1409-18.
34. Andreou A, Kopetz S, Maru DM, Chen SS, Zimmitti G, Brouquet A, Shindoh J, Curley SA, Garrett C, Overman MJ, Aloia TA, Vauthey JN. Adjuvant chemotherapy with FOLFOX for primary colorectal cancer is associated with increased somatic gene mutations and inferior survival in patients undergoing hepatectomy for metachronous liver metastases. *Ann Surg* 2012; 256: 642-50.

Accepted Article

35. Siravegna G, Bardelli A. Blood circulating tumor DNA for non-invasive genotyping of colon cancer patients. *Mol Oncol* 2016; 10: 475-80.

Table 1. Location of identified genes and allele frequency of ctDNAs at baseline.

Case ID	Gene	Chromosome	Region	Reference	Allele	Count	Coverage	MAF	COSMIC
COL-001	<i>TP53</i>	17	7578271	T	C	174	908	19.16	p.H193R
	<i>TP53</i>	17	7579349	A	G	57	269	21.19	p.F113S
COL-004	<i>PIK3CA</i>	3	178936082	G	A	21	1601	1.31	p.E542K
	<i>APC</i>	5	112175622	A	-	31	1173	2.64	-
	<i>TP53</i>	17	7574003	G	A	18	877	2.05	p.R342*
COL-015	<i>APC</i>	5	112175639	C	T	162	907	17.86	p.R1450*
	<i>PIK3CA</i>	3	178927980	T	C	63	374	16.84	p.C420R
	<i>BRAF</i>	7	140453136	A	T	67	561	11.94	p.V600E
	<i>SMARCA4</i>	19	11130307	G	A	57	870	6.55	-
	<i>APC</i>	5	112174688	G	A	42	751	5.59	-
COL-021	<i>ARID1A</i>	1	27023451..27023453	GCG	-	22	1099	2.00	-
COL-023	<i>TP53</i>	17	7577538	C	T	165	1246	13.24	p.R248Q
	<i>BRAF</i>	7	140453155	C	T	102	1114	9.16	p.D594N
	<i>APC**</i>	5	112175133^112175134	-	A	95	1056	9.00	-
COL-025	<i>SETD2**</i>	3	47162307^47162308	-	C	33	1241	2.66	-
	<i>ARID1A**</i>	1	27105676..27105678	GAA	-	24	1614	1.49	-
COL-026	<i>MET</i>	7	116399426	T	G	328	1478	22.19	-
COL-028	<i>TP53</i>	17	7577094	G	A	17	1795	0.95	p.R282W

	<i>ATM</i>	11	108205756	C	T	11	1332	0.83	p.R2691C
COL-030	<i>APC</i>	5	112175212..112175216	AAAAG	-	792	1425	55.58	p.E1309fs*4
	<i>TP53</i>	17	7578526	C	A	520	939	55.38	p.C135F
	<i>BRAF</i>	7	140453154	T	C	354	1305	27.13	p.D594G
COL-034	<i>ATM</i>	11	108098592	T	A	343	385	89.09	-
	<i>APC</i>	5	112175212..112175216	AAAAG	-	965	1094	88.21	p.E1309fs*4
	<i>NRG1</i>	8	32621340	C	T	1060	1234	85.90	-
	<i>CCND1</i>	11	69462883	C	G	401	1019	39.35	-
COL-035	<i>APC</i>	5	112174093	T	-	487	2239	21.75	p.Y935fs*20
	<i>APC</i>	5	112175639	C	T	412	2280	18.07	p.R1450*
	<i>KRAS</i>	12	25398284	C	T	302	1386	21.79	p.G12D
	<i>FBXW7</i>	4	153258983	G	A	136	1039	13.09	p.R278*
COL-041	<i>PIK3CA</i>	3	178936091	G	A	17	1416	1.2	p.E545K
	<i>APC</i>	5	112175317	A	-	12	909	1.32	-
COL-043	<i>ARID1A</i>	1	27107110..27107111	TT	-	18	1410	1.28	-
COL044	<i>PTEN</i>	10	89712014..89712017	GCAG	-	139	620	22.42	-
	<i>TSC1</i>	9	135781307	G	-	17	1096	1.55	-
COL-045	<i>FLT3</i>	13	28589808	C	T	408	940	43.4	-
	<i>PIK3CA</i>	3	178936091	G	A	371	1896	19.57	p.E545K
	<i>BRAF</i>	7	140494266^140494267	-	C	494	2545	19.41	-
COL-046	<i>BRAF</i>	7	140453193..140453194	TC	-	69	712	9.69	-

COL-051	<i>APC</i>	5	112175348..112175353	GAATTT	TCGC	385	511	79.12	-
COL-055	<i>TP53</i>	17	7578403	C	T	1676	2134	78.54	p.C44Y
	<i>FLT3</i>	13	28674628	T	C	105	220	47.72	-
	<i>MAP3K1</i>	5	56177743	G	A	666	1563	42.61	-
COL-057	<i>BRAF</i>	7	140494266^140494267	-	C	206	1555	13.25	-
	<i>TP53</i>	17	7578552	G	T	43	422	10.19	p.Y126*
COL-058	<i>APC**</i>	5	112175348	G	T	157	1362	11.53	p.E1353*
	<i>TP53</i>	17	7579849^7579850	-	GTCG AAAAAT GTTTC CT	72	884	8.14	-
	<i>SMARCA4</i>	19	11145716..11145718	GAG	-	26	1074	2.42	-
	<i>FBXW7</i>	4	153332605..153332607	CTC	-	23	1196	1.92	p.E117del
	<i>JAK1</i>	1	65306996^65306997	-	T	19	1235	1.54	-
	<i>APC</i>	5	112176673	C	-	18	1005	1.79	-
COL-060	<i>VHL</i>	3	10191642^10191643	-	GGC	42	661	6.35	-

Validation by analysis of matched tumor tissue mutation was not performed in patients COL-021, COL-026, and COL-046 for whom there was a limited amount of tissue DNA. Twenty-five (48%) out of the 52 ctDNAs were registered in the catalogue of somatic mutations in cancer (COSMIC), and the affected amino acid mutations are shown in the rightmost column. **These mutations were not detected at post-progression period.

Figure Legends

Figure 1. ctDNAs identified in plasma.

Gene mutations for which ctDNAs were identified in the plasma of 11 mCRC patients are indicated. The blue tiles indicate single nucleotide variants that cause a missense or a nonsense mutation. The green tiles indicate insertion or deletion of nucleotides. An asterisk indicates two different mutations of the same gene.

Figure 2. Changes in ctDNA levels (Mutant allele frequency [MAF]) during therapy.

The median MAF values at baseline, remission, and post-progression were 13.24 (range 0.95-89.1), 1.85 (range 0-68.6), and 9.17 (range 0-80.8), respectively (red lines). Significance was assessed using the Wilcoxon signed-rank test.

Figure 3. Correlation between MAF and tumor burden (A), CEA (B), and CA19-9 (C).

Three types of mark represent data at each time-points; white round point (○) for baseline, plus mark (+) for remission, and black round point (●) for post-progression.

Regression values for all time points are 0.57 in A (95% confidence interval [CI] 0.44 - 0.67), 0.0082 in B (95% CI -0.16 - 0.17), and 0.0036 in C (95% CI -0.16 - 0.17).

Regression values for each time point are included directly on the figures (A-C).

Figure 4. Overall survival according to the percentage reduction in MAF at the remission period.

Kaplan Meier survival curves of overall survival in patients grouped according to the percentage reduction in MAF at the remission period. The median overall survival was 32.5 months (95%CI, 25.4-not available) in the MAF <2% group and 16.6 months (95%CI, 13.2-not available) in the MAF \geq 2% group (p=0.002).

Figure 5. Clinical course of patient COL-001.

Changes in the ctDNA levels of two *TP53* mutations over the clinical course are independent of changes in the amount of total cell-free DNA (cfDNA) or tumor markers. (Top) The clinical course of the patient was followed by CT scans of liver metastases at baseline (left), remission (middle) and after progression (right). (Middle) Plasma levels of the tumor markers CA19-9 (brown) and CEA (green) were followed over the clinical course. (Bottom) Changes in two *TP53* ctDNA mutations (blue and brown) measured as % MAF, and in total cell-free DNA (cfDNA, bars) over the clinical course.

Figure 6. Newly detected mutations at post-progression.

Newly detected ctDNA mutations at post-progression (red) and ctDNA mutations detected over the entire clinical course (black) are shown for two different patients. A) The MAF of the newly detected mutation in *CREBBP* was 1.08% (number of mutant reads=19, coverage depth of the lesion=1755). B) The MAF of the newly detected mutation in *FBXW7* was 1.81% (number of mutant reads=23, coverage depth of the lesion=1271).

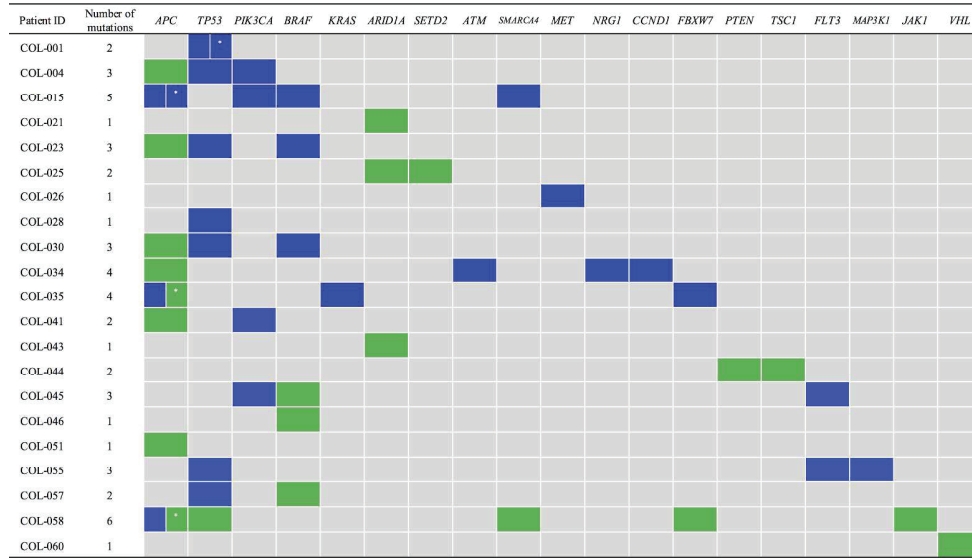


Figure 1. ctDNAs identified in plasma.

300x171mm (300 x 300 DPI)

Accepted

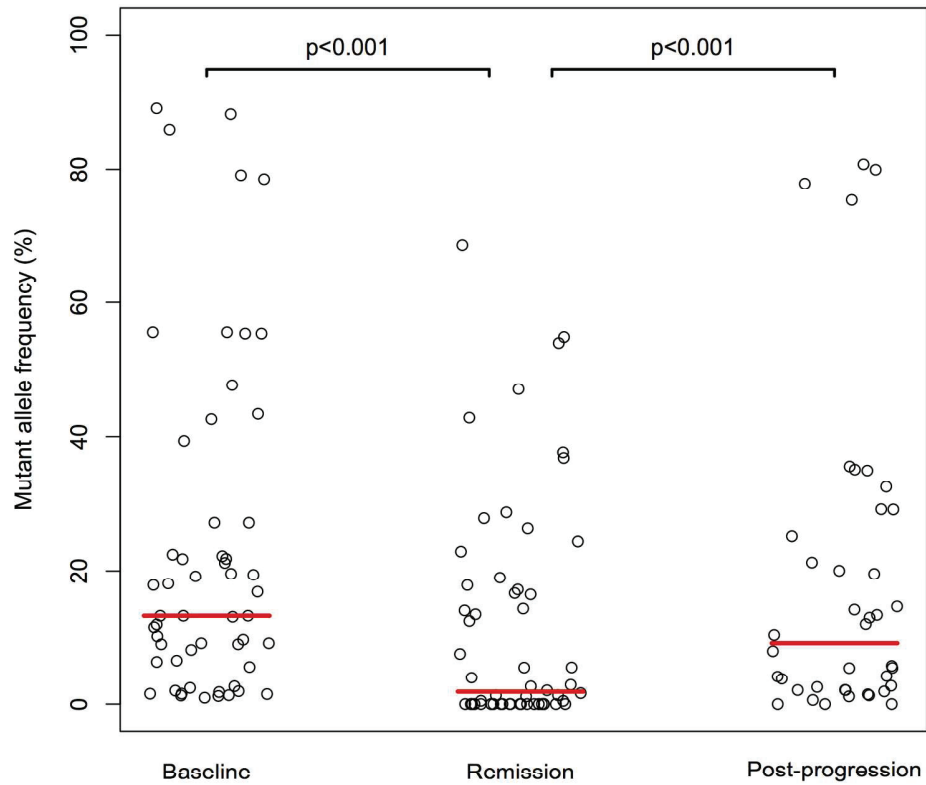


Figure 2. Changes in ctDNA levels (Mutant allele frequency [MAF]) during therapy.

177x177mm (300 x 300 DPI)

Acc

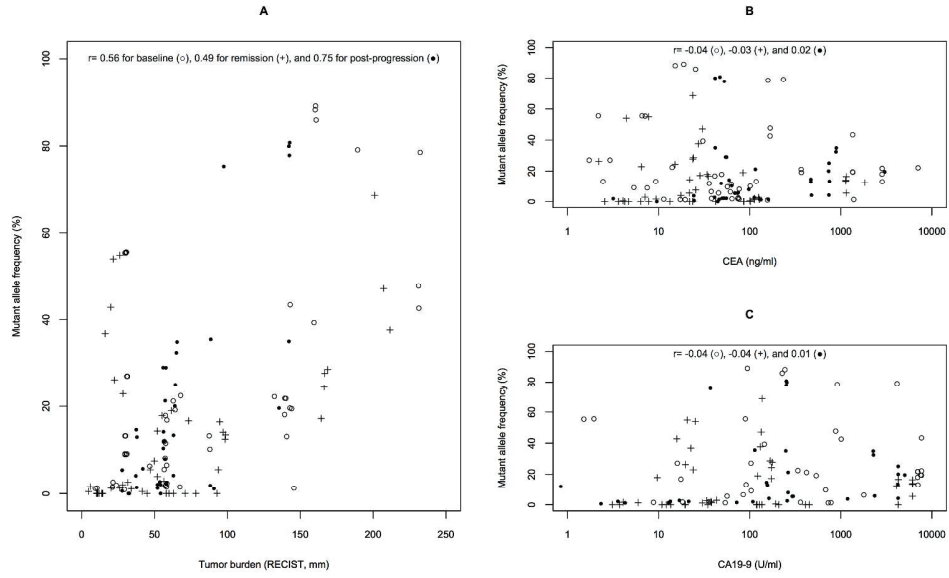


Figure 3. Correlation between MAF and tumor burden (A), CEA (B), and CA19-9 (C).

330x206mm (300 x 300 DPI)

Accepte

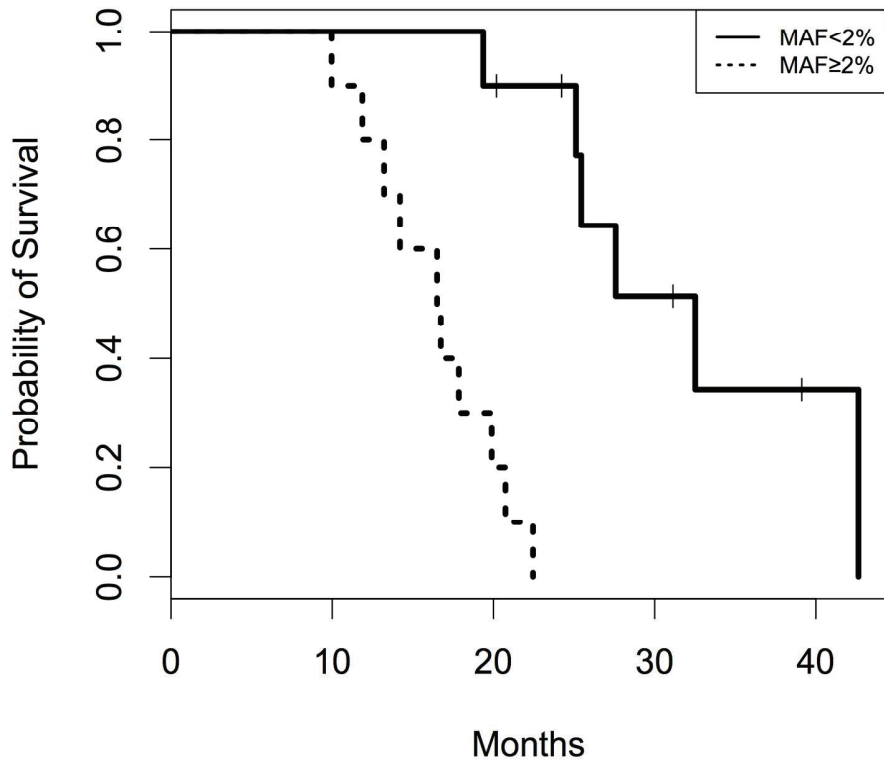


Figure 4. Overall survival according to the percentage reduction in MAF at the remission period.

177x177mm (300 x 300 DPI)

Acc

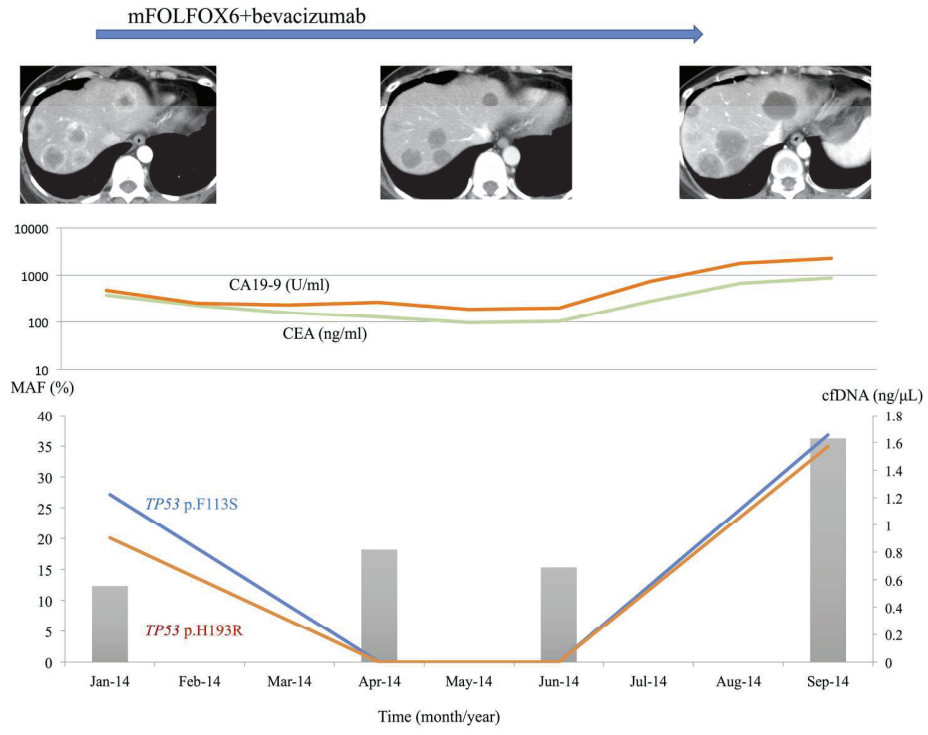


Figure 5. Clinical course of patient COL-001.

190x142mm (300 x 300 DPI)

Accepted

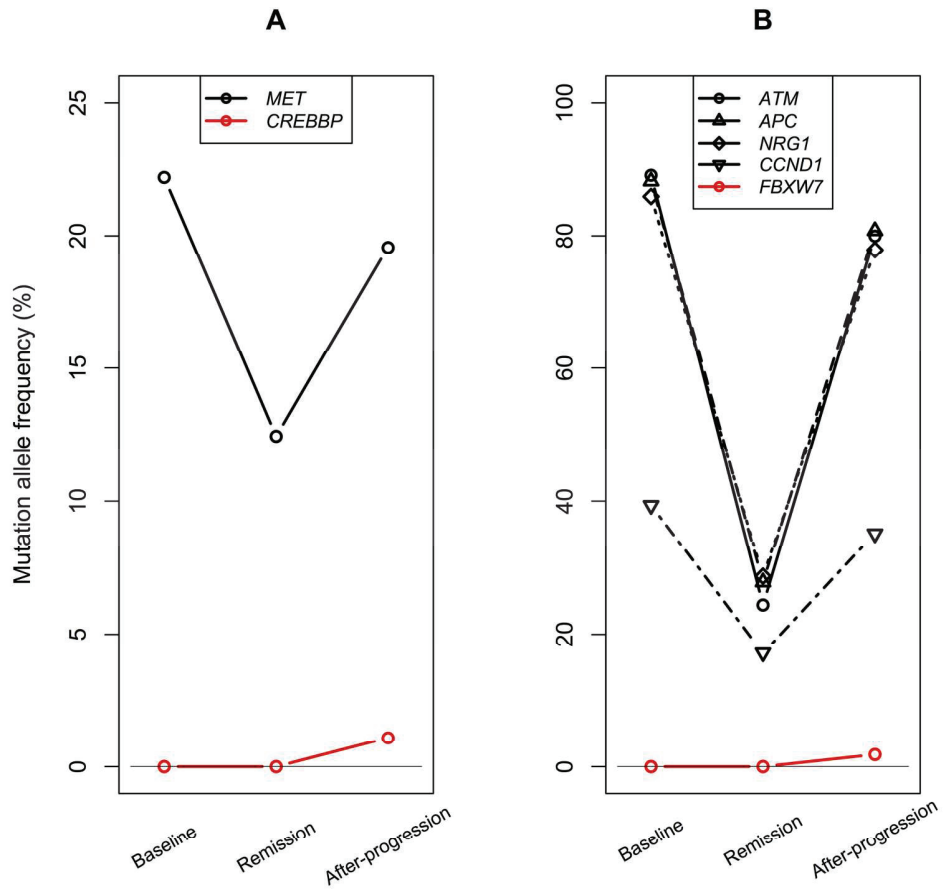


Figure 6. Newly detected mutations at post-progression.

177x177mm (300 x 300 DPI)

Acc